^{210}Po production in the European DEMO fusion reactor

Merlijn A J Mertens[1,2,3], Ulrich Fischer[1], Pavel Pereslavtsev[1], Robert Stieglitz[1], Jean-Marie Noterdaeme[4,5] and Stefaan Cottenier[2,3]

[1]Institute for Neutron Physics and Reactor Technology, Karlsruhe Institute of Technology, Hermann-von-Helmholtz Platz 1, D-76344 Eggenstein-Leopoldshafen, Germany
[2] Center for Molecular Modeling, Ghent University, Technologiepark 903, B-9052 Zwijnaarde, Belgium
[3] Department of Electrical Energy, Metals, Mechanical Construction and Systems, Ghent University, Technologiepark 903, B-9052 Zwijnaarde, Belgium
[4] Department of Applied Physics, Ghent University, Sint-Pietersnieuwstraat 84 B4, B-9000 Ghent, Belgium
[5] Max-Planck-Institut für Plasmaphysik, Boltzmannstraße 2, D-85748 Garching, Germany

E-mail: `stefaan.cottenier@ugent.be`

Abstract. The radionuclide inventory plays a central role in the safety of nuclear installations both during operation and their decommissioning. In nuclear fusion reactors using Pb-Li tritium breeding blankets, the undesired production of radiotoxic ^{210}Po is still an unresolved safety issue. In this work, neutron transport calculations and inventory calculations are combined to predict the ^{210}Po inventory in a DEMO fusion reactor using either a Helium Cooled Lithium Lead or a Water Cooled Lithium Lead breeding blanket. In order to guarantee that the environmental ^{210}Po release associated with an ex-vessel leak-of-PbLi accident remains below the no-evacuation limit, the ^{210}Po concentration in the Pb-Li should be kept below 1500 appt. It was found that no Pb-Li purification is required to keep the ^{210}Po concentration in DEMO below this limit. However, in case the Pb-Li makes direct contact with water, more volatile Po-containing (oxy-)hydroxides could form. If these species increase the ^{210}Po release rate by more than a factor two, safety measures will be required. Therefore, ^{210}Po generation in DEMO does not pose a hazard in case of a regular ex-vessel leak-of-PbLi accident, unless possibly in case the Pb-Li makes contact with water.

Keywords: breeding blanket, Pb-Li, Po-210, radiotoxic, DEMO, activation, inventory
Submitted to: *Nucl. Fusion*

1. Introduction

The first generation of commercial fusion reactors will generate electricity exploiting the deuterium-tritium (D-T) fusion reaction. The earth's oceans account for a virtually inexhaustible supply of deuterium as 0.0156 % of the hydrogen isotopes in ocean water is deuterium (according to the Vienna Standard Mean Ocean Water). Tritium, however, having a half-life of 12.32 years, only appears in trace amounts in nature. The very limited global inventory of tritium available today has been exclusively generated in CANDU-type fission reactors and is estimated to range between 12.2 and 27.6 kg at the start-up time of the European DEMO (DEMOnstration power station) fusion reactor, while its required start-up inventory is of the same order of magnitude [1]. Therefore, in order to scale up nuclear fusion to a viable and economical source of energy, a fusion reactor will have to produce (breed) at least as much tritium as it consumes. The most realistic way to do this, is by making as many fusion neutrons as possible interact with ^{6}Li, which primarily results in the production of T and ^{4}He. As it is inevitable that some fusion neutrons will interact with other materials or will simply escape from the reactor, a neutron multiplier is indispensable. The prime candidates for this purpose are Pb and Be. They both have advantages and disadvantages and are therefore still being studied in parallel.

This work addresses the undesired production of radiotoxic ^{210}Po occurring only in the tritium breeding concepts using Pb as a neutron multiplier. In these concepts, liquid eutectic Pb-Li circulates through a blanket surrounding the fusion plasma and is frequently bypassed through a Tritium Extraction and Removal System which collects the produced T. The undesired ^{210}Po production is initiated by a radiative neutron capture by ^{208}Pb, the main component of natural Pb (52.8 %). This results in ^{209}Pb which is unstable and quickly undergoes a beta decay into ^{209}Bi ($t_{1/2} = 3.25$ h). When this isotope subsequently captures another neutron, either ground state ^{210g}Bi or metastable ^{210m}Bi is produced. The latter alpha decays into ^{206}Tl ($t_{1/2} = 3.04 \times 10^{6}$ y), while the former beta decays ($t_{1/2} = 5.01$ d) into the problematic ^{210}Po which is a strong α-emitter having a specific activity of 166 TBq/g [2] (4500 times higher than ^{266}Ra) and a half-life $t_{1/2}$ of 138 days. It was found to be highly radiotoxic, with a median systemic lethal dose LD_{50} estimated in the range of only $3.773 - 21.56$ MBq ($23 - 130$ ng) for a 70-kg male adult [3, 4]. The problematic reaction chain is visualized in Figure 1.

Although ^{210}Po will not pose problems during the decommissioning phase of the fusion reactor (due to its relative short half-life), its inventory needs to be monitored during operation to ensure the safety of the workers as well as to prevent a release to the environment. The aim of this study is to obtain a realistic estimation of the Po inventory in the European DEMO fusion reactor, which, if any limit value is exceeded, may stipulate complementary safety measures or a purification system.

2. Computational tools

2.1. Geometrical model of the European DEMO reactor

Over the years, different generic models of the European DEMO reactor have been proposed by the Power Plant Physics and Technology (PPPT) programme of the EUROfusion Consortium. These reference designs contain the foreseen implementation of the major components of the reactor (vacuum vessel, magnetic field coils, divertor, etc.) and define the residual space available for the breeding blanket. In this work, the DEMO baseline configuration 'DEMO1 2014' was used for which the most important characteristics are listed in Table 1 [5]. In order to keep the computational cost reasonable, calculations are performed in a 11.25° toroidal section of this model (making optimal use of the toroidal symmetry of the model). Four breeding blanket concepts are currently being developed in the EU and are considered for implementation in the European DEMO [6]: Helium Cooled Pebble Bed (HCPB), Helium Cooled Lithium Lead (HCLL), Water Cooled Lithium Lead (WCLL) and Dual Coolant Lithium Lead (DCLL). As the name suggest, the latter three use liquid Pb-Li as breeder/multiplier combination. In this work, calculations on the HCLL and WCLL blanket designs have been performed. For both concepts, two implementations in the generic model were considered: (i) a homogeneous implementation in which the blanket models are filled by a concept-

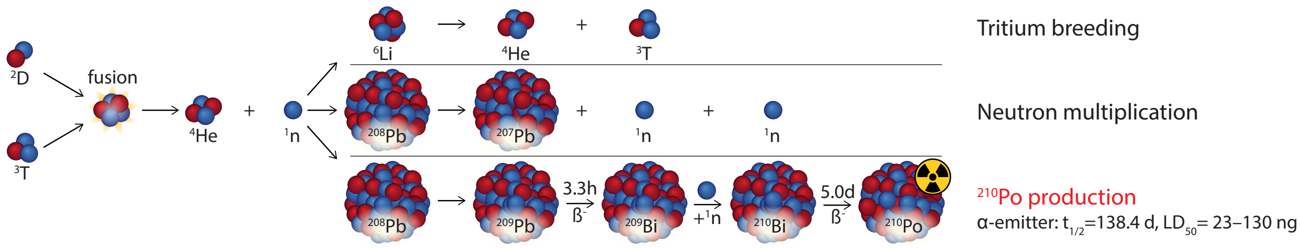

Figure 1: A visual summary of the ^{210}Po production reaction chain. The problematic reaction chain is initiated when a (fusion) neutron is captured by ^{208}Pb instead of being multiplied (lower reaction path).

specific homogeneous material mixture [7], and (ii) a heterogeneous implementation containing the concept-specific blanket module including e.g. cooling pipes and stiffening plates [8, 9]. The idea behind this approach is to examine whether a homogeneous model of the design yields results comparable to the ones obtained for a detailed heterogeneous model. If this is the case, there is no need to create a heterogeneous model for all future intermediate blanket designs (which can be time-intensive), but instead the material mixture in the homogeneous model can be adapted accordingly to acquire a good (first) estimation of the ^{210}Po inventory. Figure 2 shows a poloidal section of the models used in the calculations. In these models, the material composition of all components has been defined. This allows us to perform realistic neutron transport calculations throughout the full model and determine the neutron flux in the components where Pb-Li is present. The total amount of Pb-Li in each model is listed in Table 2. It is assumed that Li is enriched to a 90% ^{6}Li content to enhance the tritium breeding capability.

Number of TF coils	16
Major radius	9.0 m
Minor radius	2.25 m
Aspect ratio	3.6
Plasma elongation	1.56
Plasma triangularity	0.33
Fusion power	1572 MW
Average neutron wall loading	1.07 MW/m^2
Net electric power	500 MW
Fusion neutron source intensity	5.581×10^{20} n/s

Table 1: Characteristics of the 'DEMO1 2014' baseline [5].

2.2. Neutron transport calculations

To calculate the energy-dependent neutron flux in the Pb containing regions, neutron transport calculations were performed using the MCNP (Monte Carlo N-Particle) code [10], which is currently the reference

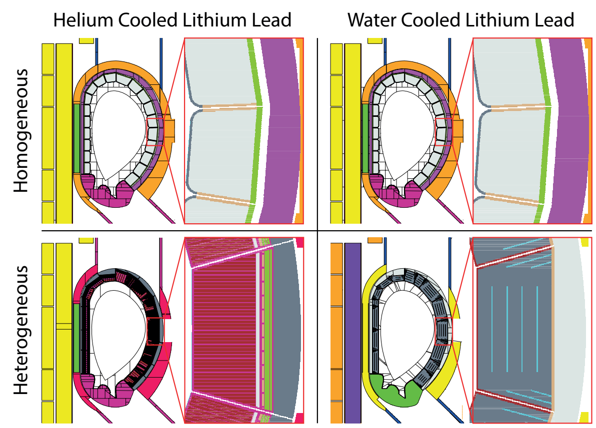

Figure 2: A poloidal section of the 4 DEMO models used in the neutron transport calculations. For each model, the equatorial outboard module is also shown in detail.

Table 2: The Pb-Li volumes implemented inside and outside the breeding zone (BZ) for the dfferent models.

$V_{\mathrm{Pb-Li}}$ (m^3)	HCLL		WCLL	
	homo.	het.	homo.	het.
Inside BB	575	563	575	668
Outside BB	150	150	150	150
Total	725	713	725	818

code for neutron transport calculations. It uses the Monte Carlo principle to probabilistically track the neutrons on a microscopic level from birth to death throughout a 3D geometry in which the material composition has been defined. Along this track, all possible physical interactions between the neutron and the material are modeled based on their probability of occurrence. A realistic fusion neutron source was used which is based on the properties of the 'DEMO1 2014' baseline (see Table 1) and a mathematical description of a typical tokamak fusion neutron source [11]. It should be noted that MCNP can not model the variation of the material composition over time resulting from transmutations. Nevertheless, the obtained initial neutron flux spectrum can be used for the whole lifetime of the reactor, as the Li burn-up and inventory build-up for a DEMO fusion reactor is quite limited, making the neutron flux spectrum approximately constant over time.

2.3. Nuclear data used in the MCNP calculations

The probability of a nuclear reaction is given by the corresponding energy-dependent cross section, which are evaluated using theoretical models (often) combined with experimentally measured cross-section data. Relying on different theoretical models, large distinctions sometimes exist between the same cross section found in different nuclear data libraries. Therefore, the choice of nuclear data library can have a significant impact on the obtained neutron flux spectrum. To allow for an unambiguous comparison of results, a common set of evaluated nuclear data for fission and fusion applications has been developed i.e. the Joint Evaluated Fission and Fusion (JEFF) nuclear library [12]. The EUROfusion project demands that all neutron transport calculations on the European DEMO are performed using this library. In this work, the JEFF-3.2 version was used.

2.4. Inventory calculation

As MCNP can not calculate the time-dependent material composition in the model, a dedicated inventory code was used for this purpose. FISPACT-II is a Fortran code developed by the United Kingdom Atomic Energy Authority allowing to perform inventory calculations [13]. The required input consists of (i) the initial density of the material, (ii) the initial chemical composition and (iii) the time-dependent neutron flux in the material. The program then allows to determine the material composition at any requested time. FISPACT-II also makes use of dedicated nuclear data libraries. In this work, ten nuclear data libraries have been compared of which four were selected for detailed calculations.

The liquid Pb-Li is not static within the breeding blanket but continuously circulates through a dedicated loop of which some parts are located close to and others far away from the fusion plasma. The loop is essentially composed of the breeding blanket modules (high neutron flux), the Pb-Li manifold (lower neutron flux) and the Pb-Li storage tank, the heat exchanger, the tritium extraction system and the pumps (negligible neutron flux). In the HCLL blanket concept the Pb-Li is foreseen to complete 11 recirculations per day, while in the WCLL about 10 recirculations per day are expected [14]. This has two important consequences on the ^{210}Po inventory: (i) all activation products are continuously redistributed over the whole Pb-Li circuit rather than remaining in the area where they were produced and (ii) not all Pb-Li is continuously being exposed to a high neutron flux, therefore areas of different neutron flux have to be distinguished.

Commercial eutectic Pb-Li available today typically contains between 10 – 33 appm ^{209}Bi impurities [15]. These impurities have an effect on the final ^{210}Po inventory as they provide a shortcut in the problematic reaction chain shown in Figure 1. The neutrons can be captured directly by ^{209}Bi, resulting in a higher ^{210}Po production rate. This effect has to be considered to decide whether it is necessary to use a higher quality “nuclear grade” Pb-Li or even an on-site Pb-Li purification system.

DEMO is foreseen to have two breeding blanket phases. In the first phase, a so-called starter blanket will be installed limited to a maximum displacement damage to the structural material of 20 dpa. For the second phase, a new blanket generation allowing for 50 dpa structural material damage is expected, based on the progress in material irradiation studies [6]. In this work, we focus on the starter blanket as this is the one currently under design. This blanket will be used during the first 5.2 years of DEMO operation and the irradiation schedule shown in Figure 3 can be assumed for the inventory calculations. In this first blanket phase, DEMO will be operated at 30% of its full power capacity for 5.173 years, followed by 48 4-hour pulses at full power with 1-hour intervals at zero power. The total lifetime of DEMO is set at 6 full-power years (FPY). A conservative irradiation schedule would therefore be a continuous operation for 6 years at full power, which can also be considered as representative for a first generation commercial fusion reactor. Both of these irradiation schedules will be simulated and compared.

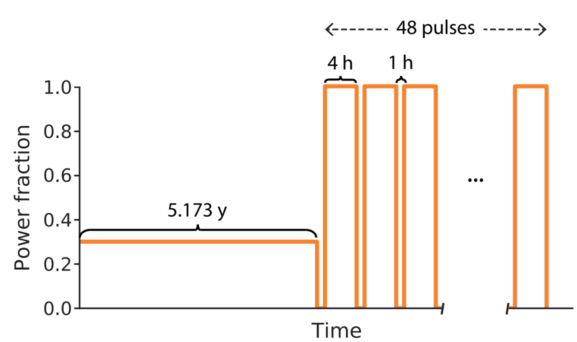

Figure 3: DEMO first blanket irradiation schedule assumed in the activation calculations.

3. Results

3.1. Neutron flux

In the MCNP neutron transport calculations several regions containing Pb-Li were distinguished. The most important ones are the actual breeding zones. In the homogeneous models, these regions refer to the entire material mixture filling the blanket modules. In the heterogeneous models, however, they refer to the regions within the blanket module that contain pure Pb-Li. It is expected that most of the ^{210}Po will be produced within these regions as they contain the largest portion of the total Pb-Li amount and are exposed to the highest neutron flux. The obtained energy-dependent neutron flux in these regions for all four models, is shown in Figure 4. It can be seen that for the WCLL blanket, a softer (less-energetic) spectrum is found due to the moderation of the neutrons by water molecules . The resulting neutron spectra in the breeding regions for the homogeneous and the heterogeneous model are found to be qualitatively the same with some distinctions at lower neutron energy for which the heterogeneous models yield a lower flux. This is because of the increased absorption rate of low-energy neutrons by ^{6}Li, which is present at larger concentrations in pure Pb-Li than in the homogeneous blanket mixtures. It should be noted that in this work not only the breeding zones were considered to be contributing to the ^{210}Po production, but also all other regions containing Pb-Li with a non-negligible neutron flux such as the Pb-Li manifold and the blanket backplate.

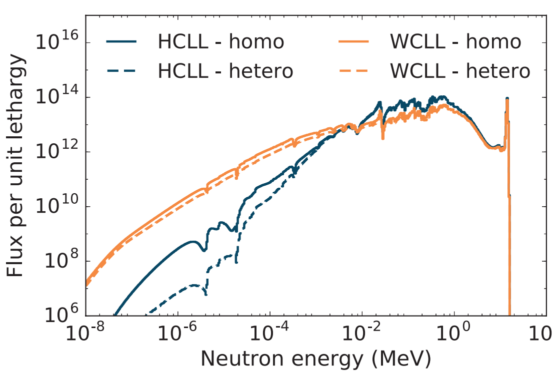

Figure 4: Calculated neutron flux spectra in the breeding zones for the 4 considered DEMO models.

3.2. Proof of instantaneous mixing assumption

The obtained neutron fluxes for the different regions containing Pb-Li were used to calculate the ^{210}Po inventory with FISPACT-II. In a first calculation only internal circulation of Pb-Li was allowed, meaning that activation products generated within a given region (breeding zone, manifold, backplate) always stayed within that same region. This results in an accumulation of activation products in the breeding zones where the neutron flux is higher than in the other regions. The increased ^{209}Bi concentration in the breeding zones promotes ^{210}Po production, resulting in a higher overall ^{210}Po inventory.

In reality however, the Pb-Li circulates through the entire Pb-Li loop at a rate specific to the breeding blanket concept. For the HCLL concept one cycle takes 2.2 hours (11 recirculations/day), while for the WCLL concept one cycle takes 2.4 hours (10 recirculations/day) [14]. A 6 FPY irradiation schedule is now considered which amounts to a total of 24107 and 21915 redistribution steps for the HCLL and WCLL designs. As simulating this large amount of redistribution steps showed to be quite demanding, at first fewer redistribution steps (and so longer redistribution intervals) are assumed. Then the number of redistribution steps is gradually increased towards the target value to study the evolution of the result. The final ^{210}Po inventory as a function of the number of redistribution steps is shown in Figure 5 (for both the EAF-2010 and TENDL-2014 nuclear data library). It can be seen that the ^{210}Po inventory has converged to a stable value long before the actual number of redistribution steps is reached. The crosses in Figure 5 were obtained assuming instantaneous mixing (using a single volume-averaged flux). It can be seen that the obtained results coincides with the converged result. Therefore, instantaneous mixing can be assumed which allows to volume-average the fluxes in the different regions. This way, more complex irradiation schedules can be considered using the available computational resources.

3.3. Comparing nuclear data for FISPACT-II

The final ^{210}Po inventory depends on the nuclear data library used in the FISPACT-II calculation. Two nuclear cross sections have a critical impact on the final result: the neutron capture cross section of ^{208}Pb and the neutron capture cross section of ^{209}Bi resulting in ground state ^{210g}Bi. To speed up the calculations, FISPACT-II collapses the energy-dependent cross sections with the specified energy-dependent neutron flux resulting in a single effective one-group (flux spectrum weighted) cross section for every type of nuclear interaction. Figure 6 shows these effective cross sections σ_{eff}, as well as the ^{210g}Bi/^{210}Bi$_{\mathrm{tot}}$ branching ratios and the final ^{210}Po inventories that were all calculated for the homogeneous HCLL neutron spectrum and the DEMO first blanket irradiation schedule using 10 different nuclear data libraries. The error bars were de-

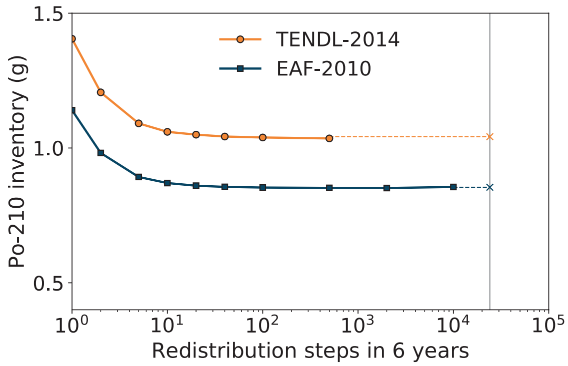

Figure 5: The calculated ^{210}Po inventory versus the number of redistribution steps used during a 6 FPY irradiation schedule for the homogeneous HCLL model for both the EAF-2010 and TENDL-2014 libraries. The gray vertical line marks the actual number of Pb-Li cycles in 6 years. The crosses and dashed lines show the obtained value assuming instantaneous mixing.

duced by FISPACT-II.

It can be seen that different versions of the same library tend to give similar results. The JENDL-4.0 library was found to give exactly the same result as the JEFF-3.3 library, which suggests that these libraries share nuclear data. The biggest discrepancies between the libraries were found to result from the different ^{209}Bi(n,g)^{210g}Bi cross section used. It can be seen that this cross section is roughly directly proportional to the presented branching ratios, proving that a consensus exists about the total neutron capture cross section of ^{209}Bi but not about the branching ratios. This issue has been addressed in detail by Fiorito et al. [16] and in conclusion they urge the need for dedicated experiments in order to remove these discrepancies. Four well established nuclear data libraries enclosing the entire range of results were selected for further calculations: the European Activation File 2010 (EAF-2010) [17], the TALYS-based Evaluated Nuclear Data Library 2017 (TENDL-2017) [18], the Joint Evaluated Fission and Fusion File 3.3 (JEFF-3.3) [12] and the U.S. Evaluated Nuclear Data File 8.0 (ENDF/B-VIII.0) [19].

3.4. ^{210}Po inventory: ^{209}Bi impurity level effect

Multiple ^{210}Po inventory calculations were performed using different initial ^{209}Bi impurity levels in the Pb-Li. A linear relationship was found between the final ^{210}Po inventory and the initial ^{209}Bi impurity level:

$$N_{^{210}\mathrm{Po}} = N^{\mathrm{no\,Bi}}_{^{210}\mathrm{Po}} + A N_{^{209}\mathrm{Bi,i}}. \quad (1)$$

In this equation, $N_{^{210}\mathrm{Po}}$ denotes the final ^{210}Po inventory for a given initial Bi impurity level $N_{^{209}\mathrm{Bi,i}}$, $N^{\mathrm{no\,Bi}}_{^{210}\mathrm{Po}}$ is the final ^{210}Po inventory for impurity-free Pb-Li and A is the determined slope. $N^{\mathrm{no\,Bi}}_{^{210}\mathrm{Po}}$ and A are presented in units of appt and appt/appm respectively in Table 3 and 4 for the DEMO first blanket irradiation schedule and in Table 5 and 6 for a 6 FPY irradiation schedule. They can also be obtained in units of mg and mg/appm by multiplying the reported values by 8.247 for the homogeneous HCLL, 8.104 for the heterogeneous HCLL, 8.242 for the homogeneous WCLL and 9.301 for the heterogeneous WCLL (these factors are obtained using the total Pb-Li volumes shown in Table 2 and an average Pb-Li density of 9500 kg/m^3 corresponding to a Pb-Li temperature of 292°C [20]).

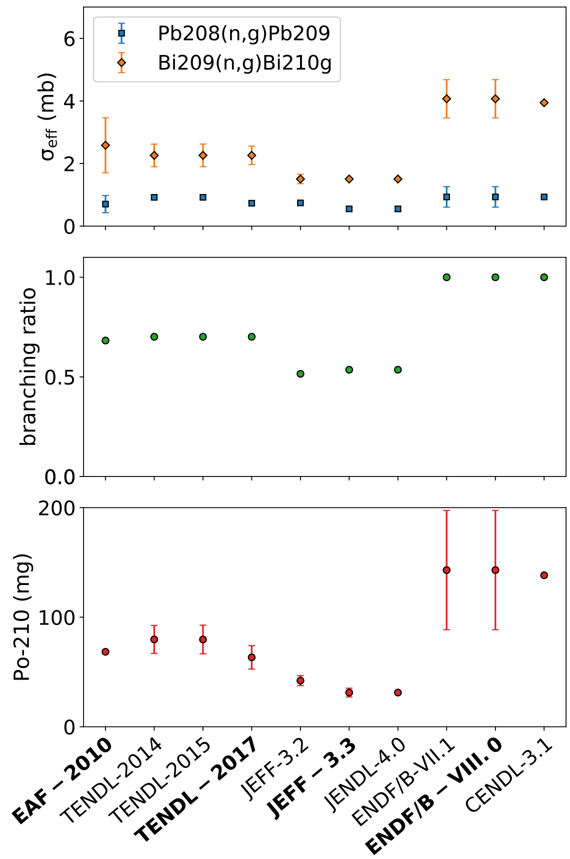

Figure 6: The effective one-group cross sections of the important neutron captures for ^{210}Po production (top), the ^{210g}Bi/^{210}Bi$_{\mathrm{tot}}$ branching ratios in case of a neutron capture by ^{209}Bi (center) and the final ^{210}Po inventories (bottom), all calculated for the homogeneous HCLL neutron flux spectrum and the DEMO first blanket irradiation schedule using 10 different nuclear data libraries.

The obtained ^{210}Po inventories are higher for the 6 FPY irradiation schedule as this is a more intensive irradiation schedule than the one foreseen for the first DEMO blankets. It can be seen that the choice of nuclear data library has a dominant impact on the resulting ^{210}Po inventory: the ENDF/B-VIII.0 library produces values up to 4.6 times (360%) higher than the ones obtained for the JEFF-3.3 library. The differences in the flux spectra obtained using the homogeneous and heterogeneous model (Figure 4) are found to have an almost negligible effect for the HCLL blanket (maximum discrepancy in the ^{210}Po concentration is only 2%), while for the WCLL blanket the effect is somewhat larger due to the larger flux at low neutron energies (where the major discrepancies are found), resulting in a ^{210}Po concentration up to 30% higher for the homogeneous model (corresponding to a total ^{210}Po inventory higher by at most 15% given the larger Pb-Li volume in the heterogeneous model, see Table 2). However, the effect remains small compared to the discrepancies introduced by using different nuclear data libraries. Therefore, it can be concluded that homogeneous models can be used to obtain a good first indication of the expected ^{210}Po inventory for future intermediate blanket designs. Nevertheless, it is advisable to use a detailed heterogeneous model to estimate the ^{210}Po inventory in the final blanket design.

For impurity-free Pb-Li, the HCLL concept is found to result in somewhat higher ^{210}Po concentrations than for the WCLL concept (see Table 3 and 5). However, the homogeneous WCLL concept is found to be more sensitive to the initial ^{209}Bi impurity level compared to the other models as can be seen from the higher slopes A (see Table 4 and 6). As a result, this model will result in the highest ^{210}Po concentrations whenever the initial ^{209}Bi concentration exceeds a given limit which varies between 1.4 and 36 appm depending on the nuclear data library and irradiation schedule.

Using the obtained coefficients of equation 1, it is now possible to calculate the ^{209}Bi impurity level corresponding to a 10 % increase in the final ^{210}Po inventory. The obtained values are presented in Table 7 and 8 for the two irradiation schedules and are a good indication for the Bi impurity level at which a noticeable impact on the final ^{210}Po inventory can be expected. All Bi impurities levels lower than the reported ones could thus be considered as having negligible impact. In case of a 6 FPY irradiation schedule, more ^{210}Po will be produced starting from ^{208}Pb compared to the first DEMO blanket irradiation schedule. This reduces the relative significance of the initial ^{209}Bi impurities present in the Pb-Li, thus resulting in higher values in Table 8. As previously mentioned, commercial eutectic Pb-Li available today typically contains between 10 – 33 appm ^{209}Bi impurities [15]. It can be seen that all values in Table 7 and 8 are lower than these values, which means that the Pb-Li should be purified before operation to at least these levels if one wants to nullify the impact of the initial Bi impurities. A similar approach can be used to calculate the Bi impurity limits for e.g. a final ^{210}Po inventory of 1 appb or a total ^{210}Po inventory of 1 g in the total Pb-Li volume.

Table 3: The final ^{210}Po inventory for a Pb-Li breeder free of ^{209}Bi impurities ($N^{\mathrm{no\,Bi}}_{^{210}\mathrm{Po}}$ in Eq. 1) in units of appt for different blanket models and nuclear data libraries and the **DEMO first blanket irradiation schedule**.

$N^{\mathrm{no\,Bi}}_{^{210}\mathrm{Po}}$ (appt)	HCLL		WCLL	
	homo.	het.	homo.	het.
EAF-2010	8.30	8.41	5.44	4.19
TENDL-2017	7.68	7.68	6.12	4.65
JEFF-3.3	3.78	3.85	2.54	1.95
ENDF/B-VIII.0	17.3	17.7	10.7	8.18

Table 4: Coefficient A from Eq. 1 in units of appt ^{210}Po per appm ^{209}Bi impurities in the Pb-Li for different blanket models and nuclear data libraries and the **DEMO first blanket irradiation schedule**.

A (appt/appm)	HCLL		WCLL	
	homo.	het.	homo.	het.
EAF-2010	2.90	2.86	3.49	2.84
TENDL-2017	2.62	2.56	3.70	2.93
JEFF-3.3	1.69	1.68	2.04	1.64
ENDF/B-VIII.0	4.56	4.53	5.26	4.28

Table 5: The final ^{210}Po inventory for a Pb-Li breeder free of ^{209}Bi impurities ($N^{\mathrm{no\,Bi}}_{^{210}\mathrm{Po}}$ in Eq. 1) in units of appt for different blanket models and nuclear data libraries and a **6 FPY irradiation schedule**.

$N^{\mathrm{no\,Bi}}_{^{210}\mathrm{Po}}$ (appt)	HCLL		WCLL	
	homo.	het.	homo.	het.
EAF-2010	104	105	67.9	52.4
TENDL-2017	99.9	100	77.8	58.9
JEFF-3.3	47.2	48.0	31.8	24.3
ENDF/B-VIII.0	216	221	133	102

3.5. Safety analysis

In 2006, Petti et al. [21] have performed a safety analysis on a conceptual 1000 MWe fusion power plant ARIES-AT. In this analysis, they estimated that in case of an ex-vessel leak-of-PbLi accident a ^{210}Po concentration of 100 appt in the eutectic Pb-Li would results in a total amount of 0.43 TBq ^{210}Po being released into the environment in the first hour after the

Table 6: Coefficient A from Eq. 1 in units of appt ^{210}Po per appm ^{209}Bi impurities in the Pb-Li for different blanket models and nuclear data libraries and a **6 FPY irradiation schedule**.

A (appt/appm)	HCLL		WCLL	
	homo.	het.	homo.	het.
EAF-2010	9.30	9.19	11.19	9.13
TENDL-2017	9.06	8.90	12.3	9.73
JEFF-3.3	5.42	5.38	6.56	5.27
ENDF/B-VIII.0	14.6	14.5	16.9	13.7

Table 7: Maximum amount of initial ^{209}Bi impurities in ppm to keep the increase in the final ^{210}Po inventory below 10 % w.r.t. Pb-Li free of impurities for different blanket models and nuclear data libraries and the **DEMO first blanket irradiation schedule**.

$N^{10\,\%}_{^{209}\mathrm{Bi,imp}}$ (ppm)	HCLL		WCLL	
	homo.	het.	homo.	het.
EAF-2010	0.286	0.294	0.156	0.147
TENDL-2017	0.293	0.300	0.165	0.158
JEFF-3.3	0.224	0.229	0.124	0.118
ENDF/B-VIII.0	0.380	0.390	0.203	0.191

Table 8: Maximum amount of initial ^{209}Bi impurities to keep the increase in the final ^{210}Po inventory below 10% w.r.t. Pb-Li free of impurities for different blanket models and nuclear data libraries and a **6 FPY irradiation schedule**.

$N^{10\,\%}_{^{209}\mathrm{Bi,imp}}$ (ppm)	HCLL		WCLL	
	homo.	het.	homo.	het.
EAF-2010	1.11	1.14	0.607	0.574
TENDL-2017	1.10	1.12	0.632	0.606
JEFF-3.3	0.872	0.892	0.484	0.461
ENDF/B-VIII.0	1.48	1.52	0.790	0.743

accident before the heating-ventilation-air conditioning system of the lower functional area (where the Pb-Li pool forms) is shut down. This quantity showed to be about half the allowable no-evacuation release limit of 0.92 TBq for a release point close to the ground, a 1 km site boundary and average weather conditions.

Consider a DEMO reactor using 'dirty' commercial Pb-Li (33 appm ^{209}Bi) and no purification system. Under these conditions, ^{210}Po inventories between 56.1 and 184 appt (depending on the nuclear data library used) are found for the DEMO first blanket irradiation schedule and between 198 and 700 appt for a 6 FPY irradiation schedule. For both cases the maximum predicted inventory is above the 100 appt limit determined for ARIES-AT. However, the ARIES-AT fusion power plant is designed to use Pb-Li both as breeder and coolant. As a result, the Pb-Li blanket outlet temperature is as high as 1125°C, which is far above the Pb-Li operation temperature foreseen for a DEMO fusion reactor using an HCLL or WCLL blanket i.e. 300°C and 328°C respectively [14, 22, 23]. Petti et al. [21] demonstrated that in case of an ex-vessel leak-of-PbLi accident at ARIES-AT, 0.64 TBq of ^{210}Po is expected to evaporate in the form of PbPo from the leaked Pb-Li pool (initially at 980°C) within the first two hours. This was found to be least 30000 times more than the amount of PbPo expected to evaporate within the first two hours in case of a leak-of-PbLi accident at DEMO, resulting in a Pb-Li pool below 300°C. This is because the PbPo mobilization rate is governed by a diffusion-limited bulk process at high temperatures, whilst being limited by a slower surface evaporation process at low temperatures.

As the surface evaporation rate is directly proportional to the ^{210}Po concentration in the Pb-Li, it could be proposed to allow ^{210}Po inventories 30000 times higher than the 100 appt limit determined for ARIES-AT. However, although PbPo is indeed expected to be the primary evaporating species in an inert atmosphere [24], recent experiments suggest that in contact with air, Po-containing (oxy-)hydroxides with a higher volatility than PbPo but lower than elementary Po will form [25]. Using the known evaporation rate of elementary Po, a conservative upper limit of the ^{210}Po amount evaporating within 2 hours from a DEMO-conditioned Pb-Li pool in contact with air was estimated and found to be still at least 15 times smaller than the evaporated PbPo amount at ARIES-AT. Therefore, a new ^{210}Po concentration limit of 1500 appt could be proposed for DEMO. In the previous paragraph, it was shown that the predicted ^{210}Po inventories for DEMO using 'dirty' Pb-Li (33 appm ^{209}Bi) are at least a factor 2 below this new limit. Therefore, ^{210}Po is expected not to pose a threat in case of a leak-of-PbLi accident in which the Pb-Li is in contact with air. It should be noted however, that in case the Pb-Li makes contact with water (e.g. the coolant in the case of WCLL), Po species more volatile than elementary Po are expected to form [25]. If these species increase the evaporation rate by more than a factor two, certain safety measures will be required. A dedicated study of the stability and volatility of these Po-containing (oxy-)hydroxides is required to make statements on the required ^{210}Po concentration threshold keeping the ^{210}Po release below the safe limit for this specific accident scenario. If the evaporation rate increases by not more than a factor 15, a safe ^{210}Po concentration threshold would be 100 appt which can be satisfied for the DEMO first blanket irradiation schedule by using relatively clean commercial

Pb-Li (< 17 appm ^{209}Bi) and for the 6 (or longer) FPY irradiation schedule by incorporating an on-site Pb-Li purification system keeping the ^{209}Bi level always below 5 appm.

4. Conclusions

Combining MCNP neutron transport calculations and FISPACT-II inventory calculations, the expected ^{210}Po inventories in the HCLL and WCLL breeding blankets for the DEMO fusion reactor have been determined. It was found that the discrepancies resulting from using different nuclear data libraries are often larger than the ones obtained for the different models. The inconsistency of the branching ratio between a neutron capture by ^{209}Bi resulting in either ^{210g}Bi or ^{210m}Bi is the primary cause and dedicated experiments are necessary. A safety analysis showed that in case of an ex-vessel leak-of-PbLi accident in DEMO, a ^{210}Po concentration below 1500 appt would limit the environmental ^{210}Po release to values below the no-evacuation limit. Even for the most conservative combination of Pb-Li purity, irradiation schedule and nuclear data library, the ^{210}Po concentration stays below this limit by at least a factor 2, with no need for Bi or Po removal from the Pb-Li. However, if the Pb-Li makes contact with water, very volatile Po-containing (oxy-)hydroxides could form. If these species increase the evaporation rate by more than a factor 2, certain safety measures will be required (e.g. on-site Pb-Li purification).

Acknowledgments

M.A.J.M. benefits from a PhD Fellowship of the Research Foundation - Flanders (FWO) and was awarded an additional travel grant by FWO to enable a research stay at KIT. M.A.J.M. acknowledges EUROfusion for granting the permission to use the MCNP DEMO models. S.C. acknowledges financial support from OCAS NV by an OCAS-endowed chair at Ghent University.

References

[1] Pearson R J, Antoniazzi A B and Nuttall W J 2018 *Fusion Engineering and Design* **136** 1140–1148 ISSN 0920-3796 URL http://www.sciencedirect.com/science/article/pii/S092037961830379X

[2] Health Physics Society 2010 Polonium-210: Contamination Information and Updates - fact sheet http://hps.org/newsandevents/polonium210.html [online; accessed 31-July-2019] URL http://hps.org/newsandevents/polonium210.html

[3] Harrison J, Leggett R, Lloyd D, Phipps A and Scott B 2007 *Journal of Radiological Protection* **27** 17–40 ISSN 0952-4746

[4] Scott B R 2007 *Dose Response* **5** 94–122 ISSN 1559-3258 URL https://www.ncbi.nlm.nih.gov/pmc/articles/PMC2477690/

[5] Federici G, Kemp R, Ward D, Bachmann C, Franke T, Gonzalez S, Lowry C, Gadomska M, Harman J, Meszaros B, Morlock C, Romanelli F and Wenninger R 2014 *Fusion Engineering and Design* **89** 882–889 ISSN 0920-3796 URL http://www.sciencedirect.com/science/article/pii/S0920379614000714

[6] Cismondi F, Boccaccini L V, Aiello G, Aubert J, Bachmann C, Barrett T, Barucca L, Bubelis E, Ciattaglia S, Del Nevo A, Diegele E, Gasparotto M, Di Gironimo G, Di Maio P A, Hernandez F, Federici G, Fernández-Berceruelo I, Franke T, Froio A, Gliss C, Keep J, Loving A, Martelli E, Maviglia F, Moscato I, Mozzillo R, Poitevin Y, Rapisarda D, Savoldi L, Tarallo A, Utili M, Vala L, Veres G and Zanino R 2018 *Fusion Engineering and Design* **136** 782–792 ISSN 0920-3796 URL http://www.sciencedirect.com/science/article/pii/S0920379618302989

[7] Eade T, Garcia M, Garcia R, Ogando F, Pereslavtsev P, Sanz J, Stankunas G and Travleev A 2017 *Fusion Engineering and Design* **124** 1241–1245 ISSN 0920-3796 URL http://www.sciencedirect.com/science/article/pii/S092037961730193X

[8] Villari R, Jaboulay J, Aiello G, Palermo I and Fischer U 2015 2014 DEMO HCLL MCNP model Internal IDM document EFDA_D_2M6MQZ EUROfusion URL https://idm.euro-fusion.org/?uid=2M6MQZ

[9] Palermo I, Fernadez I, Rosa E, Moro F and Fischer U 2015 2014 DEMO HCLL MCNP model Internal IDM document EFDA_D_2M82V3 EUROfusion URL https://idm.euro-fusion.org/?uid=2M82V3

[10] Werner C (ed) 2017 *MCNP Users Manual - Code Version 6.2* (Los Alamos National Security, LCC) ISBN LA-UR-17-29981

[11] Fischer U 2014 Guidelines for PPPT neutronic analyses Internal IDM document EFDA_D_2L8TR9 v1.7 EUROfusion URL https://idm.euro-fusion.org/?uid=2L8TR9

[12] Nuclear Energy Agency 2017 JEFF Nuclear Data Library https://www.oecd-nea.org/dbdata/jeff/ [online, accessed 31-July-2019] URL https://www.oecd-nea.org/dbdata/jeff/

[13] Sublet J C, Eastwood J W, Morgan J G, Gilbert M R, Fleming M and Arter W 2017 *Nuclear Data Sheets* **139** 77–137 ISSN 0090-3752 URL http://www.sciencedirect.com/science/article/pii/S0090375217300029

[14] Utili M, Tincani A, Candido L, Savoldi L, Zanino R, Zucchetti M, Martelli D and Venturini A 2019 *IEEE Transactions on Plasma Science* **47** 1464–1471

[15] Conde E, Barrado A I, Pascual L, Fernández M, Salazar J M G d, Barrena M I and Quiñones J 2014 *Fusion Engineering and Design* **89** 1246–1250 ISSN 0920-3796 URL http://www.sciencedirect.com/science/article/pii/S0920379614002634

[16] Fiorito L, Stankovskiy A, Hernandez-Solis A, Eynde G V d and Zerovnik G 2018 *EPJ Nuclear Sciences & Technologies* **4** 48 ISSN 2491-9292 URL https://www.epj-n.org/articles/epjn/abs/2018/01/epjn170080/epjn170080.html

[17] Sublet J C, Packer L W, Kopecky J, Forrest R A, Koning A J and Rochman D A 2010 The european activation file: Eaf-2010 neutron-induced cross section library Tech. Rep. CCFE-R (10) 05 Culham, UK

[18] 2017 TENDL-2017 nuclear data library https://tendl.web.psi.ch/tendl_2017/tendl2017.html [online; accessed 31-July-2019] URL https://tendl.web.psi.ch/tendl_2017/tendl2017.html

[19] Brown D A, Chadwick M B, Capote R, Kahler A C, Trkov A, Herman M W, Sonzogni A A, Danon Y, Carlson A D,

Dunn M, Smith D L, Hale G M, Arbanas G, Arcilla R, Bates C R, Beck B, Becker B, Brown F, Casperson R J, Conlin J, Cullen D E, Descalle M A, Firestone R, Gaines T, Guber K H, Hawari A I, Holmes J, Johnson T D, Kawano T, Kiedrowski B C, Koning A J, Kopecky S, Leal L, Lestone J P, Lubitz C, Márquez Damián J I, Mattoon C M, McCutchan E A, Mughabghab S, Navratil P, Neudecker D, Nobre G P A, Noguere G, Paris M, Pigni M T, Plompen A J, Pritychenko B, Pronyaev V G, Roubtsov D, Rochman D, Romano P, Schillebeeckx P, Simakov S, Sin M, Sirakov I, Sleaford B, Sobes V, Soukhovitskii E S, Stetcu I, Talou P, Thompson I, van der Marck S, Welser-Sherrill L, Wiarda D, White M, Wormald J L, Wright R Q, Zerkle M, Žerovnik G and Zhu Y 2018 *Nuclear Data Sheets* **148** 1–142 ISSN 0090-3752 URL http://www.sciencedirect.com/science/article/pii/S0090375218300206

[20] Schulz B 1991 *Fusion Engineering and Design* **14** 199–205 ISSN 0920-3796 URL http://www.sciencedirect.com/science/article/pii/0920379691900028

[21] Petti D A, Merrill B J, Moore R L, Longhurst G R, El-Guebaly L, Mogahed E, Henderson D, Wilson P and Abdou A 2006 *Fusion Engineering and Design* **80** 111–137 ISSN 0920-3796 URL http://www.sciencedirect.com/science/article/pii/S0920379605004199

[22] Utili M, Bassini S, Boccaccini L, Bühler L, Cismondi F, Del Nevo A, Eboli M, DiFonzo F, Hernandez T, Wulf S, Kordač M, Martelli D, De les Valls E M, Melichar T, Mistrangelo C, Tarantino M, Tincani A and Vála L 2019 *Fusion Engineering and Design* ISSN 0920-3796 [in press; published online May. 2019] URL http://www.sciencedirect.com/science/article/pii/S0920379619306143

[23] Utili M 2015 Preliminary model T transport in bu for hcll and wcll - intermediate report Tech. Rep. EFDA_D_2M89QE EUROfusion URL https://idm.euro-fusion.org/?uid=2M89QE

[24] Mertens M A J, Aerts A, Infante I, Neuhausen J and Cottenier S 2019 *Journal of Physical Chemistry Letters* **10** 2879–2884 ISSN 1948-7185 (*Preprint* https://doi.org/10.1021/acs.jpclett.9b00824) URL https://doi.org/10.1021/acs.jpclett.9b00824

[25] Maugeri E A, Neuhausen J, Eichler R, Piguet D, Mendonça T M, Stora T and Schumann D 2014 *Journal of Nuclear Materials* **450** 292–298 ISSN 0022-3115 URL http://www.sciencedirect.com/science/article/pii/S0022311513012610